Journal of Computational Applied Mechanics 2024, 55(3): 473-484

DOI: 10.22059/jcamech.2024.376537.1090

RESEARCH PAPER

Spectral method for modeling the Dispersion of complex guided wave modes in anisotropic pipeline

Zitouni Ismaine [a, *], Rhimini Hassan [a], Chouaf Abdelkerim [a]

[a] *Laboratory of Mechanics, Engineering and Innovation (LM2I) National High School of Electricity and Mechanics Casablanca, Morocco*

Abstract

Ultrasonic guided waves play a crucial role in the non-destructive testing of pipelines. Their dispersive nature and the diversity of modes present make them often difficult to interpret, especially in areas close to defects or when transducers are located close to the edges. In these situations, in addition to propagative modes, complex modes also appear. The aim of this study is to use the spectral method to plot the dispersion curves of ultrasonic guided waves in anisotropic pipelines.

We begin by describing the mathematical formulation of the problem, then explain and apply the spectral method algorithm to plot these curves, covering different levels of anisotropy in order to test the robustness of the method to various mechanical behaviors. Particular attention is paid to complex modes, which are poorly studied in the pipeline literature. We treated longitudinal and torsional modes. This study enables us to understand the frequency ranges that favor the appearance of these modes.

The results obtained are compared with analytical solutions based on classical algorithms. We also compare the computation time and coding effort required with those of previous analytical methods. These studies demonstrate the significant advantage of the spectral method in terms of accuracy, efficiency and computation time savings for plotting the dispersion curves of complex modes in anisotropic pipelines.

Keywords: Ultrasonic guided waves; spectral method; dispersion curve; pipeline; complex modes.

Corresponding author: *ismaine.zitouni.doc20@ensem.ac.ma

1. Introduction

Ultrasonic guided waves (UGW) have established themselves as an essential inspection tool in the field of non-destructive testing. Their ability to propagate over long distances without significant attenuation, while inducing a global vibration of the waveguide, makes them one of the most widely used waves for inspecting the health of large flat and cylindrical structures [1,2]. To carry out non-destructive testing using UGW and study the interaction of the wave with a defect, several elements are required. Among these essential elements are the dispersion curves and the shape of the mode to be generated. From a mathematical point of view, dispersion curves represent the pairs (frequencies, wavenumbers) that satisfy the dispersion equations. From a physical point of view, they indicate the

[*] Corresponding author. *E-mail address:* ismaine.zitouni.doc20@ensem.ac.ma

frequencies likely to generate UGW in a given waveguide. Using these curves, we can obtain information on the different modes that can be generated, as well as their cut-off frequencies. The frequencies thus obtained are classified into two families, depending on the vibratory state of the controlled structure (symmetrical or non-symmetrical vibration). The study of UGW dispersion began decades ago and is still of great importance today. These curves can be obtained either analytically, using function root finding techniques (such as the Newton-Raphson method [3], the bisection method [4] and hybrid methods [5]), or using numerical methods and information from numerical simulations [6], or experimentally [7].

Numerous analytical studies have been carried out by various researchers to mathematically formulate and plot the dispersion curves of various types of waveguides. These include Gazis [8,9], Graff [10] and Nayfeh [11,12]. Others have explored the asymptotic analysis of dispersion equations to simplify calculations [13,14]. However, these formulations become complex when dealing with multilayer structures (due to poor matrix conditioning). To overcome this difficulty, researchers have developed new matrix techniques for plotting dispersion curves. These include the transfer matrix method TMM [15], the stiffness matrix method SMM [16], the global matrix method GMM [17], the equivalent matrix method EM [18], the reverberant ray matrix method MRRM [19] and the effective stiffness matrix method ESM [20].

Despite the variety of analytical approaches, these remain computationally time-consuming. Numerical methods have been introduced to overcome this limitation. These include the semi-analytical finite element method (SAFE) [21], Legendre's orthogonal polynomial series method [22], as well as numerical software and free interfaces such as DISPERSE [23], DC [24,25] and GUIGUW [26]. One particular method is based on a scheme of spectral approximation of partial derivatives using the Chebyshev polynomial, known as the Spectral Method (SM). Adamou [27] developed it to characterize the dispersion of ultrasonic guided waves in cylindrical geometries with high attenuation, inhomogeneity and anisotropy. The method is based on a wavenumber-dependent formulation. Using Matlab's eig function, Adamou obtained the eigenfrequencies of the system. Karpfinger et al [28,29] extended the method to cylindrical multilayer structures. They also proposed a calculation algorithm based on the spectral method to obtain dispersion curves for a cylindrical tube with a borehole and a fluid flowing through it. Baohua Yu et al and Zharkinov et al [30,31] used MS to process multilayer cylindrical structures with imperfect contact and filled with fluid. Quintanilla [32,33] used the spectral method to characterize the dispersion of propagative and evanescent modes in highly anisotropic viscoelastic structures such as plates and cylinders. For this, he considered a frequency formulation and used a matrix method to generate the wave numbers (pure real, pure imaginary and complex). Li et al [34] treated the case of a rotating annular plate with a functional gradient of material properties varying continuously in the radial direction. Dubuc et al [35] dealt with anisotropic elastic plates under non-uniform stresses (taking into account the dispersion of propagative and non-propagative modes). Zitouni et al. [36,37] carried out a comparative study between the spectral method and analytical algorithms for finding the zero of a function. They also analyzed the eigenvectors (displacements) derived from the SM and compared them with the analytical displacements and stresses normalized by sound power. They also dealt with the case of non-propagating modes for composite plates and steel pipelines, where they proposed a hybrid method for plotting the dispersion curves of complex modes [38]. Mekkaoui et al [39] tried to optimize the spectral method by a balancing algorithm to plot the dispersion curves of multilayer structures with a large number of layers. Although the spectral method is recognized for its importance and power, it remains relatively little used in the field of guided wave propagation compared with other numerical methods. In addition, the plotting of complex modes using the spectral method is still poorly explored and lacks in-depth detail.

The aim of our work is to apply the spectral method and demonstrate its advantages over standard methods for plotting the dispersion curves of anisotropic pipelines. It also seeks to understand the dispersive behavior of complex modes in these pipelines. A better understanding of these phenomena will enable controllers to better apprehend the interactions of guided waves, particularly in the near-field of defects, thus simplifying the process of detecting and analyzing structural anomalies. To this end, the mathematical formulation of the problem is explained. We then detail and apply the spectral method algorithm to plot dispersion curves. These curves are plotted for different degrees of anisotropy (isotropic and orthotropic) and different type of materials (Nickel and Carbon fiber composite), to demonstrate the robustness of the method to different mechanical behaviors. We have chosen to deal with the case of complex modes, which are poorly treated in the literature in the case of pipelines. These modes have the characteristic of propagating in areas close to defects and in areas where waves interact with the edges of a waveguide. Both longitudinal and torsional modes were investigated. The results obtained are compared with those found analytically. A comparison of the computation time between the spectral method and previous analytical methods is implemented. Coding efforts and the number of iterations for each method are also discussed. An error calculation is demonstrated to show the conformity of the MS results. The spectral method offers a great advantage in terms of saving computation time, with high accuracy in plotting the dispersion curves of complex modes in anisotropic pipelines.

2. Mathematical formulation

The motion of an anisotropic homogeneous elastic solid can be characterized by the tensor equations of dynamic behavior [8,11]. The displacement field is expressed for a cylindrical pipe as follows:

$$\begin{cases} u_r = U_1^m(\mathrm{r})\eta_1(\mathrm{m}\theta)e^{i(k_3^m x_3-\omega t)} \\ u_\theta = U_2^m(\mathrm{r})\eta_2(\mathrm{m}\theta)e^{i(k_3^m x_3-\omega t)} \\ u_3 = U_3^m(\mathrm{r})\eta_1(\mathrm{m}\theta)e^{i(k_3^m x_3-\omega t)} \end{cases} \tag{1}$$

where U_1^m, U_2^m, U_3^m represent the radial components, η_1, η_2 are the circumferential components, ω is the angular frequency and m is a positive integer representing the order of the circumferential modes.

The expressions for the radial and circumferential components are:

$$\begin{cases} \eta_1 = \cos(\mathrm{m}\theta) \\ \eta_2 = \sin(\mathrm{m}\theta) \\ U_1^m = \dfrac{\partial\varphi}{\partial r} - \dfrac{ik_3(\varphi_2+\varphi_3)}{2} + \dfrac{ik_3(\varphi_2-\varphi_3)}{2} + \dfrac{m\varphi_1}{r} \\ U_2^m = -\dfrac{\partial\varphi_1}{\partial r} + \dfrac{ik_3(\varphi_2+\varphi_3)}{2} + \dfrac{ik_3(\varphi_2-\varphi_3)}{2} - \dfrac{m\varphi}{r} \\ U_3^m = \dfrac{1}{ik_3}(-k_3^2\varphi + \dfrac{1}{2}(\dfrac{\partial}{\partial r} + \dfrac{1-m}{2})ik_3(\varphi_2+\varphi_3) - \dfrac{1}{2}(\dfrac{\partial}{\partial r} + \dfrac{1+m}{2})ik_3(\varphi_2-\varphi_3)) \end{cases} \tag{2}$$

Where φ, φ_1, φ_2 and φ_3 are unknown functions linked only to r.

The components of the elastic pipeline stress tensor can be obtained using the behavior law and the deformation-displacement relationship written as:

$$\frac{\partial\sigma_{\mathrm{ij}}}{\partial x_{\mathrm{i}}} = \rho\frac{\partial^2 u_{\mathrm{i}}}{\partial t^2} \tag{3}$$

$$\sigma_{\mathrm{ij}} = c_{ijkl}\varepsilon_{\mathrm{kl}} \tag{4}$$

$$\varepsilon_{\mathrm{kl}} = \frac{1}{2}(\frac{\partial u_{\mathrm{k}}}{\partial x_{\mathrm{l}}} + \frac{\partial u_{\mathrm{l}}}{\partial x_{\mathrm{k}}}) \tag{5}$$

where i,j,k,l (not italicized)=1,2,3. ρ is the density, C_{ijkl} the stiffness tensor, σ_{ij} the stress tensor and ε_{kl} the strain tensor. In order to facilitate indexing notation, we adopt the following contracted notation: 1→11, 2→22, 3→33, 4→23, 5→13 and 6→12.

If we replace (1), (4) and (5) in (2) we obtain a differential equation system governed by the first- and second-order partial derivative with respect to the component r ($\frac{\partial}{\partial r}, \frac{\partial^2}{\partial r^2}$). In case of isotropic pipeline, the stresses σ_{rr},$\sigma_{r\theta}$ and σ_{r3} are written as:

$$\begin{cases} \sigma_{rr} = \lambda(\dfrac{\partial u_r}{\partial r} + \dfrac{u_r}{r} + \dfrac{1}{r}\dfrac{\partial u_\theta}{\partial\theta} + \dfrac{\partial u_3}{\partial x_3}) + 2\mu\dfrac{\partial u_r}{\partial r} \\ \sigma_{r\theta} = \mu(\dfrac{1}{r}\dfrac{\partial u_r}{\partial\theta} + \dfrac{\partial u_\theta}{\partial r} - \dfrac{u_\theta}{r}) \\ \sigma_{r3} = \mu(\dfrac{\partial u_3}{\partial r} + \dfrac{\partial u_r}{\partial x_3}) \end{cases} \tag{6}$$

Substituting equation (6) and (1) using (2) in (3) we find matrix system written as:

$$\begin{cases} (\frac{\partial^2}{\partial r^2}+\frac{1}{r}\frac{\partial}{\partial r}-\frac{m^2}{r^2}+\frac{w^2}{c_1^2})\varphi = \mathrm{k}_3^2\,\varphi \\ (\frac{\partial^2}{\partial r^2}+\frac{1}{r}\frac{\partial}{\partial r}-\frac{(m-1)^2}{r^2}+\frac{w^2}{c_1^2})h_1 = \mathrm{k}_3^2\,h_1 \\ (\frac{\partial^2}{\partial r^2}+\frac{1}{r}\frac{\partial}{\partial r}-\frac{(m+1)^2}{r^2}+\frac{w^2}{c_2^2})h_2 = \mathrm{k}_3^2\,h_2 \\ (\frac{\partial^2}{\partial r^2}+\frac{1}{r}\frac{\partial}{\partial r}-\frac{m^2}{r^2}+\frac{w^2}{c_2^2})h_3 = \mathrm{k}_3^2\,h_3 \end{cases} \tag{6}$$

with $c_1^2=\frac{\lambda+2\mu}{\rho}$, $c_2^2=\frac{\mu}{\rho}$, $h_1=\varphi_2+\varphi_3$ and $h_2=\varphi_2-\varphi_3$.

In previous works, several types of approaches have been proposed to formulate the eigenvalue and eigenvector problem. In the following, we will present the frequency approach, which has been shown to be robust for modeling UGW propagation in plates and laminates [36,37].

The frequency approach considers wavenumber to be the eigenvalue to look for, so we can write:

$$[L(\mathrm{w})]\{U\}=k_3{}^2\{U\} \tag{5}$$

Where $\{U\}=\{\varphi,h_1,h_2,h_3\}^T$ is the vector of displacement components. [L] represents diagonal matrix (4,4) matrix containing all the mathematical ($\frac{\partial}{\partial r},\frac{\partial^2}{\partial r^2}$) and physical (w,C_{ij}) aspects of the problem.

Similarly, the boundary conditions can be written as follows:

$$[L'(\mathrm{w})]\{U(\pm\frac{h}{2})\}=0 \tag{6}$$

Once the three equations of motion and the boundary conditions have been defined, the next step is to use the spectral method to solve our system.

3. Spectral method algorithm

The spectral collocation method involves discretizing the waveguide using N points distributed non-uniformly along its thickness, which we refer to as collocation points. We then substitute the partial derivatives with differentiation matrices (DMs). We opt for Chebyshev's differentiation matrices [40], recognized for their high spectral convergence. These matrices are defined from the N collocation points mentioned above, making them by size (N,N). As the equations in question contain only first- and second-order partial derivatives, we obtain first- and second-order differentiation matrices.

$$\frac{\partial^{(p)}}{\partial r^{(p)}}=[DM_{cheb}]^p_{(N,N)} \tag{7}$$

Where p is the order of the partial derivative.

We replace the approximation (7) in the equations of motion (5) and boundary conditions (6). The matrix dimensions then become $[L]_{(4N,4N)}$, $[L']_{(3N,4N)}$ and $\{U\}_{(4N,1)}$. Note that for expressions that do not contain a partial derivative, it is necessary to multiply by an identity matrix $[I]_{(N,N)}$ (for dimensional equivalence).

Figure 1 summarizes all the steps explained above:

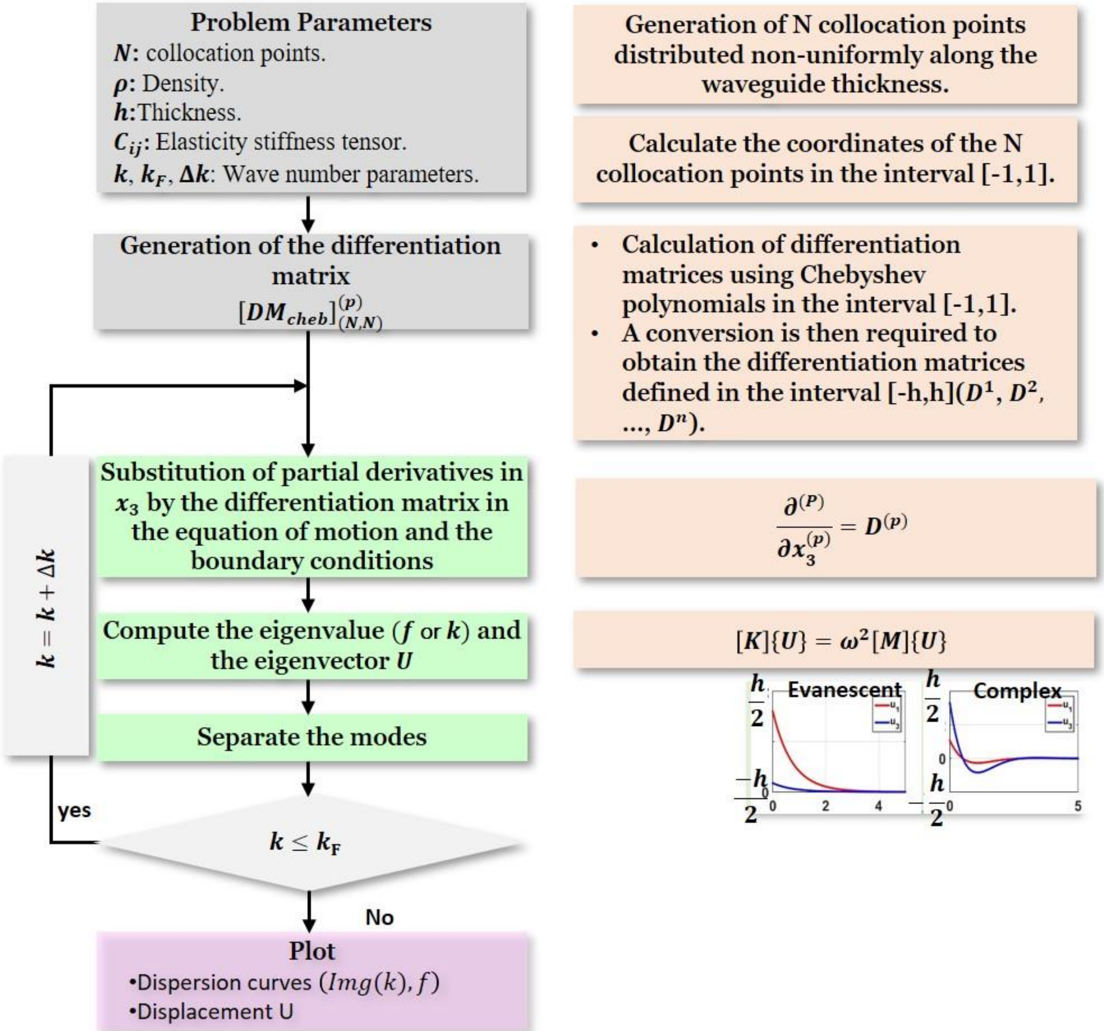

Fig 1: Flowchart of the spectral method for plotting dispersion curves for propagative, evanescent and complex modes.

The components of the matrix [L] can be written as:

$$
\begin{cases}
L_{11} = D^{(2)} + diag(\frac{1}{r})D^{(1)} - m^2 diag(\frac{1}{r^2}) + \frac{w^2}{c_1^2} I \\
L_{22} = D^{(2)} + diag(\frac{1}{r})D^{(1)} - (m-1)^2 diag(\frac{1}{r^2}) + \frac{w^2}{c_1^2} I \\
L_{33} = D^{(2)} + diag(\frac{1}{r})D^{(1)} - (m+1)^2 diag(\frac{1}{r^2}) + \frac{w^2}{c_2^2} I \\
L_{44} = D^{(2)} + diag(\frac{1}{r})D^{(1)} - m^2 diag(\frac{1}{r^2}) + \frac{w^2}{c_2^2} I
\end{cases} \tag{8}
$$

In the same way, applying the spectral method to the boundary conditions, we find:

$$
\begin{cases}
L'_{11} = -\lambda \frac{w^2}{c_1^2} I + 2\mu D^{(2)} + 2\mu m[diag(\frac{1}{r})D^{(1)} - diag(\frac{1}{r^2})] \\
L'_{22} = \mu[-2\,\mathrm{m}(\mathrm{diag}(\frac{1}{r})D^{(1)} - \mathrm{diag}(\frac{1}{r^2})) + D^{(2)} + (-D^{(1)} + D^{(1)} diag(\frac{1}{r}) - m^2 diag(\frac{1}{r^2}))] \\
L'_{33} = \frac{\mu}{2}(-2\,\mathrm{mdiag}(\frac{1}{r})D^{(1)} + (m-1) diag(\frac{1}{r^2}) + L_{22} - L_{33}) - \mu m(\mathrm{diag}(\frac{1}{r})D^{(2)} + \mathrm{diag}(\frac{1}{r^2})D^{(1)} - \mathrm{m}^2\mathrm{diag}(1/r^3) + \frac{w^2}{c_2^2}\mathrm{diag}(\frac{1}{r})) - EPS
\end{cases} \tag{9}
$$

where $EPS = 2\mu(D^{(3)} + \mathrm{diag}(\frac{1}{r})D^{(2)} - (\mathrm{m}^2+1)\,\mathrm{diag}(\frac{1}{r^2})D^{(1)} + 2\,\mathrm{m}^2\mathrm{diag}(\frac{1}{r^3})\frac{w^2}{c_1^2}D^{(1)})$.

4. Numerical results

4.1. Nomenclature of modes

We consider a homogeneous cylindrical tube unlimited along x_3 with inner radius r_1 and outer radius r_2. The cylinder is marked in coordinates (x_r,x_Θ,x_3) (Fig 2). Rotation between the cylindrical reference frame and the reference frame (x_1,x_2,x_3) takes place at an angle Θ.

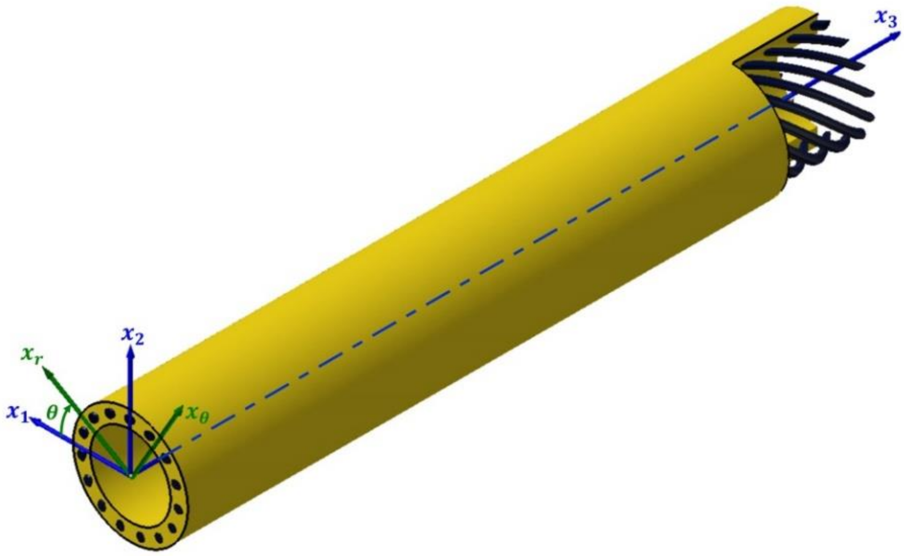

Fig 2: Pipeline geometry (x_1,x_2,x_3): Cartesian coordinate system. (x_r,x_Θ,x_3): Global cylindrical coordinate system. x_3: direction of propagation. Θ: angle between global cylindrical coordinate system and Cartesian coordinate system.

The researchers opted for a two-part approach to the study of hollow cylinders, due to the diversity of modes present. The first examines the cylinder's circumference, modeling its structure as a cylindrical ring.

The other aspect of the study focuses on the cylinder's revolution. In this case, the structure is modeled as a bar. What's remarkable here is that for certain ratios between the cylinder's thickness and its inner radius (notably at the thin plate limit), the results obtained resemble those of a plate.

The propagative modes that exist in cylindrical tubes are longitudinal modes L(0,n) (comparable to symmetrical Lamb modes for plate), torsional modes T(0,n) (comparable to SH modes) and flexural modes F(0,n).

n represents the mode number.

4.2. Nickel pipeline

Consider a nickel pipeline of thickness e=4mm. Nickel material is widely used in the production and transport of industrial gases and liquefied natural gas, which require nickel/iron alloys. The table below shows the elastic constants of this material.

Table 1: Nickel's elastic constants and density [24].

ρ(Kg/m^3)	$C_{11}=C_{22}=C_{33}$ (GPa)	$C_{12}=C_{13}=C_{23}$ (GPa)	$C_{44}=C_{55}=C_{66}$ (GPa)
8910	261	151	130.9

We then plot the pipeline dispersion curves using the spectral method for a complex wavenumber range k=i10^{-5}:10i:12000i (m^{-1}). Figure 3 shows these curves for N=15 collocation points. Figure 3a shows the complex longitudinal modes and figure 3b the complex Torsional modes. The red color designates the frequencies of the modes that propagate symmetrically along the pipeline thickness, and those in blue propagate antisymmetrically. These curves are plotted in the (frequency*thickness, wavenumber) plane. We note that we have a braiding phenomenon in the curves of figure 3a, which is in agreement with the literature for complex modes. Moreover, the complex modes increase with frequency until they reach a maximum, after which they decrease and we can observe a plane of symmetry at Imag(k)=0. These remarks are in accordance with those in the reference [41].

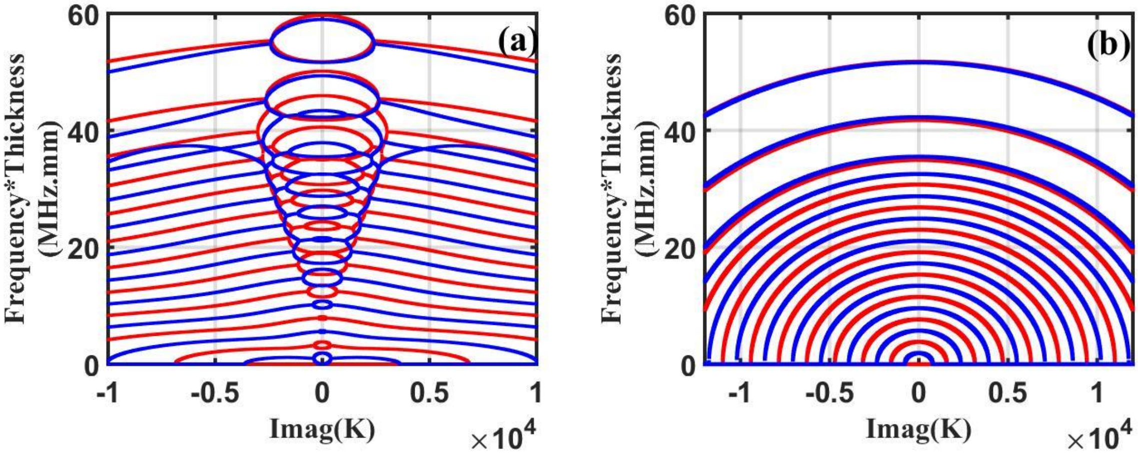

Fig 3: Dispersion curves for a Nickel pipeline plotted using the spectral method for Longitudinal modes (a) and torsional modes (b). Red color: Symmetrical modes. Blue color: Antisymmetric modes.

The spectral method was able to represent the dispersion of UGW in a material with a low degree of anisotropy (isotropic) in the following we will examine the effectiveness of SM by considering a material with a high degree of anisotropy (orthotropic).

4.3. Carbon fiber composite pipeline

We now consider a carbon fiber composite pipeline. This type of material is known for its high mechanical properties and light weight. It is widely used in the automotive and aerospace industries. The characteristics of this material are given in the following table:

Table 2: Elastic constants and density of carbon fiber composite [24].

ρ(Kg/m^3)	C_{11} (GPa)	$C_{12}=C_{13}$ (GPa)	C_{23} (GPa)	$C_{22}=C_{33}$ (GPa)	C_{44} (GPa)	$C_{55}=C_{66}$ (GPa)
1530	135	5.7	8.51	14.2	2.87	4.55

We then plot the dispersion curves of a carbon fiber composite using the spectral method for N=15. Figure 4a shows the curves for longitudinal modes and Figure 4b those for torsional modes. In the same way, we can see that the complex modes increase with frequency up to a maximum value. The maximum frequencies of longitudinal modes are greater than those of torsional modes. In addition, we have a plane of symmetry at imag(k)=0. Comparing longitudinal modes in the isotropic pipeline with those in the composite pipeline, we find that the number of modes increases with the degree of anisotropy of the material, which is normal. Moreover, even the shape of the latter changes when increasing the degree of anisotropy.

5. Discussion

To demonstrate the accuracy of the results obtained by the spectral method, we compared the eigenvalues obtained by the SM with those of the analytical method, which uses the bisection method to plot the results. The tables below show the error between the two solutions.

From Tables 3, 4, 5 and 6 we can see that the errors obtained between the bisection and spectral methods are approximately 10^{-5} for the different modes (longitudinal and symmetrical and antisymmetrical torsion) and for the two types of pipelines studied. These values are very acceptable and demonstrate the accuracy of the spectral method results. We then present a comparison table between the spectral method and two analytical reference methods (the bisection method and the Newton-Raphson method). This comparison includes computation time and number of iterations.

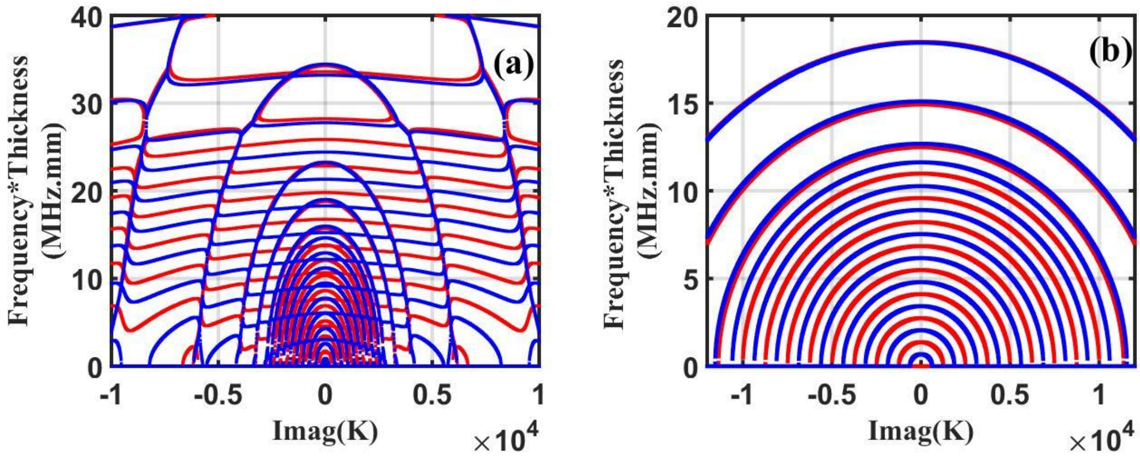

Fig 4: Dispersion curves for a carbon fiber composite pipeline plotted using the Longitudinal mode spectral method (a) and torsional mode spectral method (b). Red color: Symmetrical modes. Blue: Antisymmetric modes.

Table 3: Squared error between spectral solutions and analytical solutions of the Nickel pipeline for Longitudinal modes and Re(k)=100 m^{-1}.

Modes	Spectral frequency (fs) in MHz	Analytic frequency (fa) in MHz	Err=√(fs-fa)^2
First Symmetrical Longitudinal mode	0.680000	0.680001	1 10^{-5}
First Antisymmetrical Longitudinal mode	0.472002	0.472007	5 10^{-6}
Second symmetrical Longitudinal mode	1.929008	1.929090	8.2 10^{-5}
Second Antisymmetrical longitudinal mode	1.372501	1.372502	1 10^{-6}

Table 4: Squared error between spectral solutions and analytical solutions of the Nickel pipeline for torsional modes and Re(k)=100 m^{-1}.

Modes	Spectral frequency (fs) in MHz	Analytic frequency (fa) in MHz	Err=√(fs-fa)^2
First Symmetrical Torsional mode	0.956374	0.956323	1.7 10^{-6}
First Antisymmetrical torsional mode	0.475304	0.475314	1 10^{-5}
Second Symmetrical Torsional mode	1.915512	1.915515	3 10^{-6}
Second Antisymmetrical Torsional mode	1.436029	1.436091	6.2 10^{-5}

Table 5: Squared error between spectral solutions and analytical solutions of the composite pipeline for Longitudinal modes and Re(k)=100 m^{-1}.

Modes	Spectral frequency (fs) in MHz	Analytic frequency (fa) in MHz	$Err=\sqrt{(fs-fa)^2}$
First Symmetrical Longitudinal mode	0.392555	0.392544	$1.1\ 10^{-5}$
First Antisymmetrical Longitudinal mode	0.151561	0.151514	$4.7\ 10^{-5}$
Second Symmetrical longitudinal mode	0.850049	0.850091	$4.2\ 10^{-5}$
Second Antisymmetrical longitudinal mode	0.631238	0.631223	$1.5\ 10^{-5}$

Table 6: Squared error between spectral solutions and analytical solutions of the composite pipeline for torsional modes and Re(k)=100 m^{-1}.

Modes	Spectral frequency (fs) in MHz	Analytic frequency (fa) in MHz	$Err=\sqrt{(fs-fa)^2}$
First Symmetrical Torsional mode	0.341366	0.341362	$4\ 10^{-6}$
First Antisymmetrical Torsional mode	0.168946	0.168943	$3\ 10^{-6}$
Second Symmetrical Torsional mode	0.684377	0.684322	$5.5\ 10^{-5}$
Second Antisymmetrical Torsional mode	0.512887	0.512890	$3\ 10^{-6}$

Table 7: Comparison of different methods for the pipelines studied with a wave number calculation range k=i10^{-5}:10i:12000i (m^{-1}).

Materials	Control	Spectral method (N=15)	Bisection method	Newton-Raphson method
Steel pipeline	**Calculation time in (s)**	3.6158	2884	1598
	Number of iterations	1200 (1 for each k)	70289	94617
Carbon fiber composite pipeline	**Calculation time in (s)**	4.5406	3666	2263
	Number of iterations	1200 (1 for each k)	85721	97149

The results in Table 7 show the computational time saved when using the spectral method compared with known analytical methods for the Nickel and Carbon fiber composite pipelines. The results in Table 7 were obtained using an Intel(R) Core (TM) i5-6300U CPU @ 2.40GHz 2.50 GHz. The spectral method demonstrated its effectiveness in modeling the dispersion of ultrasonic guided waves in isotropic and anisotropic pipelines, with a saving in computation time, low coding effort and good convergence of the order of 10^{-5} compared with analytical methods based on root finding algorithms.

6. Conclusion

The aim of our study was to apply the spectral method to plot dispersion curves for anisotropic pipelines. After presenting the mathematical formulation of the problem, we used the spectral method algorithm to obtain these curves. We focused on complex modes. We varied the degree of anisotropy to demonstrate the robustness of the method to different mechanical behaviors, with particular emphasis on the treatment of complex modes, little explored in the pipeline literature. We have noted the braiding phenomenon specific to complex modes, with the different planes of symmetry represented by the dispersion curves and their extremums. Both longitudinal and torsional modes were treated. The results were compared with analytical solutions, and an analysis of computation time, error and coding effort between the spectral method and previous analytical methods was carried out. This comparison revealed a significant advantage of the spectral method in terms of computational efficiency, offering high accuracy in plotting the dispersion curves of complex modes in anisotropic pipelines. On the one hand, this study aims to show the advantages of the spectral method over conventional methods for plotting the dispersion curves of anisotropic pipelines. On the other hand, the study also aims to understand the dispersive character of complex modes in pipelines. This will make it easier for controllers to understand the interaction phenomena of guided waves, especially in the near-field of a defect. All these results encourage us in future work to apply SM in viscoelastic materials that exhibit attenuation of guided waves.

Acknowledgements

On behalf of all the authors, the corresponding author declares that there is no conflict of interest in the research, authorship, and publication of this paper.
The author(s) received no financial support for the research, authorship, and publication of this article.

References

[1] Auld, B. A., 1973, *Acoustic fields and waves in solids*, Standford university, John Wiley & sons, Рипол Классик.

[2] Achenbach, J. A., & Achenbach, J. D., 2003. *Reciprocity in elastodynamics*, Cambridge University Press, United Kingdom, library of congress Cataloging in publication data.

[3] Zitouni, I., Rhimini, H., & Chouaf, A., A Combined Newton–Bisection Approach for Calculating the Dispersion Curves in Anisotropic Multilayered Waveguides, *Journal of Vibration Engineering & Technologies*, Vol.12, No.3, pp. 1-13, 2023/11/14, 2023.

[4] ZITOUNI, Ismaine, RHIMINI, Hassan, et CHOUAF, Abdelkerim. *Modeling the Propagation of Ultrasonic Guided Waves in Four-Layer Laminated Composites*. In: International Congress for Applied Mechanics. Cham: Springer Nature Switzerland, pp. 25-33, 2022.

[5] ZITOUNI, I., RHIMINI, H., et CHOUAF, *A. Calculation of Dispersion Curves in the Composite Graphite-Epoxy Plate by a Hybrid Analytic Method*. In: International Moroccan Congress of Mechanics. Cham: Springer Nature Switzerland, 2022. pp. 3-12, 2022.

[6] CHEN, Qi, XU, Kailiang, et TA, Dean. High-resolution Lamb waves dispersion curves estimation and elastic property inversion, *Ultrasonics*, Vol. 115, pp. 106427, 2021/04/16, 2021.

[7] LIN, Jinyun, LI, Jian, JIANG, Can, et al, Theoretical and experimental investigation of circumferential guided waves in orthotropic annuli, *Ultrasonics*, Vol. 123, pp. 106715, 2022/02/21, 2022.

[8] GAZIS, Denos C., Three-dimensional investigation of the propagation of waves in hollow circular cylinders. I. Analytical foundation, *The journal of the Acoustical Society of America*, Vol. 31, No 5, pp. 568-573,1959/05, 1959.

[9] GAZIS, Denos C., Three-dimensional investigation of the propagation of waves in hollow circular cylinders. II. Numerical results, *The Journal of the Acoustical Society of America*, Vol. 31, No 5, pp. 573-578, 1959/05, 1959.

[10] Graff, K. F., 2012, *Wave motion in elastic solids*, Courier Corporation, USA, Ohio State University Press.

[11] NAYFEH Adnan H., The propagation of horizontally polarized shear waves in multilayered anisotropic media, *The Journal of the Acoustical Society of America*, Vol. 86, No 5, pp. 2007-2012, 1989/11, 1989.

[18] MONNIER, Thomas, Lamb waves-based impact damage monitoring of a stiffened aircraft panel using piezoelectric transducers, *Journal of Intelligent Material Systems and Structures*, Vol. 17, No 5, pp. 411-421, 2006/05, 2006.

[19] LI, Qiangqiang, GUO, Yongqiang, et WANG, Yajun, Analysis of Floquet waves in periodic multilayered isotropic media with the method of reverberation-ray matrix. *Crystals*, Vol. 12, No 7, pp. 904, 2022/06/24, 2022..

[20] NANDYALA, Anvesh R., DARPE, Ashish K., et SINGH, Satinder P, Effective stiffness matrix method for predicting the dispersion curves in general anisotropic composites, *Archive of Applied Mechanics*, Vol. 89, pp. 1923-1938, 2019/04/22, 2019.

[21] AZKOUR, Mustapha, EL ALLAMI, Mhammed, et RHIMINI, Hassan, Calculation of the Dispersion Curves Modeling the Propagation of Ultrasonic Lamb Waves in a Bonded Aluminum/Epoxy/Aluminum Structure Using the Semi-Analytical Finite Element Method. *Engineering Transactions*, In press, 2024/03/19, 2024.

[22] YU, J. G., ZHANG, B., LEFEBVRE, Jean-Etienne, et al, Wave propagation in functionally graded piezoelectric rods with rectangular cross-section, *Archives of Mechanics*, Vol. 67, No 3, pp. 213-231, 2015/03/24, 2015.

[23] PAVLAKOVIC, Brian, LOWE, Mike, ALLEYNE, David, et al, Disperse: A general purpose program for creating dispersion curves. *Review of Progress in Quantitative Nondestructive Evaluation*, Vol.16A, pp. 185-192, 1997.

[24] HUBER, Armin et SAUSE, Markus GR, Classification of solutions for guided waves in anisotropic composites with large numbers of layers, *The Journal of the Acoustical Society of America*, Vol. 144, No 6, pp. 3236-3251, 2018/12, 2018.

[25] Huber, A., *Dispersion Calculator*, electronic library - Dispersion Calculator (dlr.de), 2018/11/06, 2018.

[26] BOCCHINI, Paolo, MARZANI, Alessandro, et VIOLA, Erasmo, Graphical user interface for guided acoustic waves, *Journal of Computing in Civil Engineering*, Vol. 25, No 3, pp. 202-210,2011/07/19, 2011.

[27] ADAMOU, A. T. I. et CRASTER, R. V, Spectral methods for modelling guided waves in elastic media, *The Journal of the Acoustical Society of America*, Vol. 116, No 3, pp. 1524-1535, 2004/09/07, 2004.

[28] KARPFINGER, Florian, GUREVICH, Boris, et BAKULIN, Andrey, Modeling of wave dispersion along cylindrical structures using the spectral method, *The Journal of the Acoustical Society of America*, Vol. 124, No 2, pp. 859-865, 2008/08/01, 2008.

[29] KARPFINGER, Florian, VALERO, Henri-Pierre, GUREVICH, Boris, et al, Spectral-method algorithm for modeling dispersion of acoustic modes in elastic cylindrical structures, *Geophysics*, Vol. 75, No 3, pp. H19-H27, 2010/05, 2010.

[30] YU, Baohua, YANG, Shixi, GAN, Chunbiao, et al, A new procedure for exploring the dispersion characteristics of longitudinal guided waves in a multi-layered tube with a weak interface, *Journal of Nondestructive Evaluation*, Vol. 32, pp. 263-276, 2013/04/03, 2013.

[31] ZHARNIKOV, T. V., SYRESIN, D. E., et HSU, C.-J., Calculating the spectrum of anisotropic waveguides using a spectral method, *The Journal of the Acoustical Society of America*, Vol. 134, No 3, pp. 1739-1753, 2013/09/01, 2013.

[32] QUINTANILLA, F. Hernando, LOWE, M. J. S., et CRASTER, R. V., Modeling guided elastic waves in generally anisotropic media using a spectral collocation method, *The Journal of the Acoustical Society of America*, Vol. 137, No 3, pp. 1180-1194, 2015/03/01, 2015.

[33] QUINTANILLA, F. Hernando, LOWE, M. J. S., et CRASTER, R. V., Full 3D dispersion curve solutions for guided waves in generally anisotropic media, *Journal of Sound and Vibration*, Vol. 363, pp. 545-559, 2016/11/21, 2016.

[34] LI, C. L., HAN, Q., LIU, Y. J., *et al.*, Guided wave propagation in rotating functionally graded annular plates, *Acta Mechanica*, Vol. 228, pp. 1083-1095, 2017/11/17, 2017.

[35] DUBUC, Brennan, EBRAHIMKHANLOU, Arvin, et SALAMONE, Salvatore, Computation of propagating and non-propagating guided modes in nonuniformly stressed plates using spectral methods, *The Journal of the Acoustical Society of America*, Vol. 143, No 6, pp. 3220-3230, 2018/06 ,2018.

[36] ZITOUNI, Ismaine, RHIMINI, Hassan, et CHOUAF, Abdelkerim, Comparative Study of the Spectral Method, DISPERSE and Other Classical Methods for Plotting the Dispersion Curves in Anisotropic Plates, *Journal of Applied and Computational Mechanics*, Vol. 9, No 4, pp. 955-973, 2023/03/22, 2023.

[37] ZITOUNI, I., RHIMINI, H., & CHOUAF, A., Modeling the Propagation of Ultrasonic Guided Waves in a Composite Plate by a Spectral Approximation Method, *Engineering Transactions*, Vol. 71, No 2, pp. 213–227, 2023/03/05, 2023.

[38] Ismaine, Z., Hassan, R., & Abdelkerim, C., New spectral displacement post-processing approach for modeling ultrasonic guided waves. *In 2023 3rd International Conference on Innovative Research in Applied Science, Engineering and Technology (IRASET)*, IEEE, (pp. 1-8), 2023, May.

[39] MEKKAOUI, Moussa, NISSABOURI, Salah, et RHIMINI, Hassan, Towards an Optimization of the Spectral Collocation Method with a New Balancing Algorithm for Plotting Dispersion Curves of Composites with Large Numbers of Layers, *Journal of Applied and Computational Mechanics*, In press, 2024/04/29, 2024..

[40] Trefethen, L. N., 2000, *Spectral methods in MATLAB*, Society for industrial and applied mathematics, USA..

[41] Giurgiutiu, V., & Faisal Haider, M., Propagating, evanescent, and complex wavenumber guided waves in high-performance composites? *Materials*, Vol. 12, No 2, pp. 269, 2019/01/15, 2019.